

Sulfate-Functionalized Carbon/ Metal-Oxide Nanocomposites from Hydrotalcite-like Compounds

Z. P. Xu, R. Xu, and H. C. Zeng*

*Department of Chemical and Environmental Engineering, Faculty of Engineering, and
Chemical and Process Engineering Center, National University of Singapore,
10 Kent Ridge Crescent, Singapore 119260*

Received June 14, 2001; Revised Manuscript Received October 15, 2001

ABSTRACT

As a new application of hydrotalcite-like compounds, sulfate-functionalized carbon/metal-oxide nanocomposites have been prepared at relatively low temperatures in a single step, in which interlayer sulfonated polymeric anions are catalytically converted to the nanocarbons (secondary phase) while CoAl-containing brucite-like sheets are converted to the metal oxide matrices. The chemical composition and structure of nanocomposites can be controlled via selecting chemical functional groups in the intercalated polymeric anions and varying processing conditions.

In recent years, the investigation of layered double hydroxide materials (LDHs, anionic clays) becomes an active field in layered materials research owing to their many important applications.^{1–5} Among the LDHs, hydrotalcite-like compounds (HTLcs) have attracted great attention due to their synthetic flexibility in preparing catalyst and ceramic precursors and in tailor-making adsorbents, medicine stabilizers, and ion exchangers.^{1–7} In the HTLcs, both divalent and trivalent cations are located in the center of oxygen octahedra formed by six hydroxyl groups of the two-dimensional brucite-like sheets.^{1–2} To balance the extra charges carried by trivalent cations, anions have to be intercalated into the interbrucite-like sheet space (interlayer space) during the synthesis, which leads to the formation of a sandwich-like structure alternately stacked in the vertical direction of the sheets (*c*-axis), forming a 3D structure.^{1–3}

Figure 1 illustrates a schematic view of transition-metal-containing hydrotalcite-like compounds studied in this work. Considering this polymeric anion-pillared HTlc, we realize that the compound actually composes itself an organic–inorganic layered hybrid. In particular, both metal hydroxide layers (i.e., brucite-like sheets) and anion layers (in interlayer space) can be considered as starting reagents for possible solid-state reactions. Upon thermal treatment, the brucite-like sheets will be decomposed into metal oxides, which can also serve as in-situ generated catalysts, while the intercalated polymeric anions may be catalytically converted into a secondary component to metal oxide matrices. Indeed, very

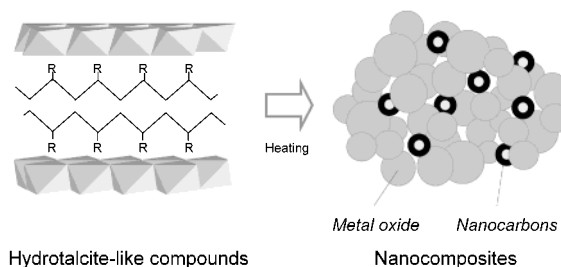


Figure 1. Schematic representation of the single-step nanocomposite synthesis via thermal decomposition of (poly)vinyl sulfonate-HTlc sample ($R = -SO_3^-$).

recently, we found that the thermal decomposition temperature of a class of newly synthesized CoMgAl-HTLcs decreases as the content of cobalt increases; the catalytic effect of cobalt on nanocarbon (with an internal cavity) formation had thus been confirmed.⁸ In this letter, we extend our previous work to include polymeric anions that bear chemical functional groups on their long hydrocarbon backbones. In this method, the alternately arranged cobalt-containing brucite-like sheet (catalyst) and the polymeric anion layer (reactant) are “blended” at the molecular level (Figure 1) for the synthesis of sulfate-functionalized carbon/metal-oxide nanocomposites.^{9,10}

The (poly)vinyl sulfonate containing CoAl-hydrotalcite-like compound was synthesized by coprecipitation of 20 mL nitrate salt solutions ($Co^{+2}/Al^{+3} = 2:1$, 1.0 M for total metal ions) in 100 mL ammoniacal solution ($[NH_3 \cdot H_2O] = 0.5$ M) mixed with sodium–(poly)vinyl sulfonate (Na–PVS; Aldrich, $[-SO_3^-]$ (in PVS) = 0.2 M) and then aging at 65

* To whom correspondence should be addressed. Tel: +65 874 2896. Telefax: +65 779 1936. E-mail: chezhc@nus.edu.sg.

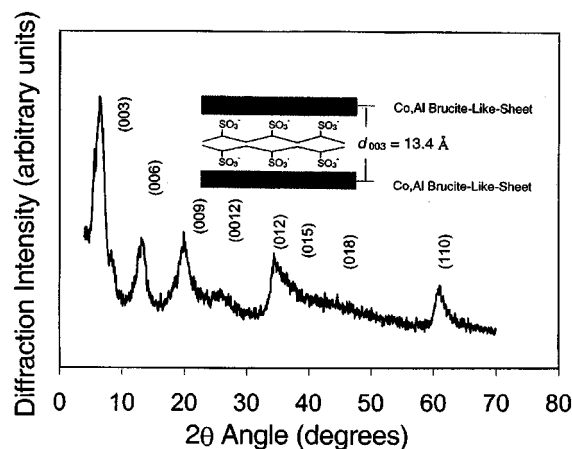


Figure 2. XRD pattern for (poly)vinyl sulfonate-HTlc sample ($\text{Co}_{0.67}\text{Al}_{0.35}(\text{OH})_2(-\text{CH}_2\text{CHSO}_3^-)_{0.40} \cdot 0.7\text{H}_2\text{O}$).

$^{\circ}\text{C}$ for 18 h under N_2 bubbling, followed by filtration and washing several times with hot deionized water ($70\text{--}80\text{ }^{\circ}\text{C}$) to remove excess PVS, the precipitate was also dried in vacuo overnight. The obtained (poly)vinyl sulfonate-HTlc was calcined respectively under flowing purified air or nitrogen (40 mL min^{-1}) for 2 h at $400\text{ }^{\circ}\text{C}$. The heated samples ($\sim 50\text{ mg}$ each) were also treated with 10 mL of 2.0 M HCl solution under gentle heating to dissolve the matrices of metal oxides, followed by thorough washing with deionized water; this purification process gives black residues that contain carbon nanoparticles (CNPs) for all the heated samples.^{11,12}

Structures of the (poly)vinyl sulfonate-HTlc and its decomposed products (sulfate-functionalized carbon/metal-oxide nanocomposites) were investigated by the X-ray diffraction method (XRD; Shimadzu XRD 6000, $\text{Cu K}\alpha$ radiation). Sample chemical analysis was carried out with inductively coupled plasma measurements (ICP; Perkin-Elmer ICP OPTIMA-3000), CHNS analysis (Perkin-Elmer 2400 CHNS analyzer), thermogravimetric analysis (TGA; Shimadzu TGA-50), Fourier transform infrared spectroscopy (FTIR; Bio-Rad, KBr pellet technique), and X-ray photoelectron spectroscopy (XPS; AXIS Hsi-165-Ultra, Kratos, $\text{Al K}\alpha$ 1486.8 eV , analyzer pass-energy at 20.0 eV). The acid-separated CNPs were also characterized with high-resolution transmission electron microscopy (HRTEM; Philips FEG CM300, at 300 kV).

The XRD pattern of as-prepared (poly)vinyl sulfonate-HTlc is displayed in Figure 2, which indicates the precipitate is indeed in the hydrotalcite phase. Different from the vertical pillaring of $[\text{C}_6\text{H}_4(\text{COO})_2]^{2-}$,^{8,13} the polymeric anions $[-\text{CH}_2\text{CHSO}_3^-]_n$ lie horizontally owing to the long hydrocarbon chains. The nearest interbrucite-like sheet distance (d_{003}) is estimated to be 13.4 \AA , which is almost identical to that reported in the literature for a PVS-pillared CoAl -hydrotalcite-like precipitate ($d_{003} = 13.3\text{ \AA}$; its experimental procedure was not given and the chemical formula of the precipitate was not determined).¹⁴ On the basis of ICP/CHNS/TGA investigation, the chemical formula for this (poly)vinyl sulfonate-HTlc can be written $\text{Co}_{0.67}\text{Al}_{0.35}(\text{OH})_2(-\text{CH}_2\text{CHSO}_3^-)_{0.40} \cdot 0.7\text{H}_2\text{O}$.

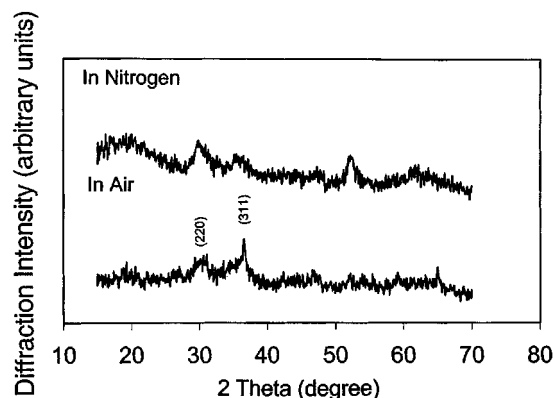


Figure 3. XRD patterns for nanocomposites prepared by heating (poly)vinyl sulfonate-HTlc sample ($\text{Co}_{0.67}\text{Al}_{0.35}(\text{OH})_2(-\text{CH}_2\text{CHSO}_3^-)_{0.40} \cdot 0.7\text{H}_2\text{O}$) respectively in nitrogen and air at $400\text{ }^{\circ}\text{C}$ for 2 h.

Table 1: FWHM Analysis for Metal Oxide Matrices in the Nanocomposites Prepared at $400\text{ }^{\circ}\text{C}$ for 2 h

| phase | crystallite size (in air) ^a | phase | crystallite size (in N_2) ^a |
|--------|--|-----------|---|
| spinel | (220) $\sim 5\text{ nm}^b$ (311) $\sim 8\text{ nm}^b$ | amorphous | $< 5\text{ nm}$ |

^a Calcined at $400\text{ }^{\circ}\text{C}$ for 2 h. ^b Crystallite size calculated from respective diffraction peaks.

As shown in Figure 3 and Table 1, XRD investigation on $400\text{ }^{\circ}\text{C}$ -heated (poly)vinyl sulfonate-HTlc sample indicates that the structural phase of the metal oxides can be selected by choosing suitable calcination atmospheres. For example, oxidative gas stream (air) gives a cubic spinel phase of $\text{Co}^{\text{II}}\text{Co}^{\text{III}}\text{Al}_{2-x}\text{O}_4$ ($x \approx 1$, based on the Co/Al ratio in the as-prepared (poly)vinyl sulfonate-HTlc) in which cobalt cations are in mixed oxidation states of $+2$ and $+3$, and inert stream (N_2) results in amorphous Co^{+2} -doped alumina.^{15–17} These observations suggest that the cobalt cations act as the catalyst for the formation of CNPs in the decomposition of the functionalized polymeric anions. Although these reactions take place within the solid phase, the same catalytic role of the low valence state metals has been observed in vapor-phase growths of CNPs, in which partially reduced cobalt oxides are attributed to the active catalytic component responsible for the formation of CNPs in the solid–vapor interface.^{11,12,18,19}

An analysis of XRD diffraction peaks (full-width-at-half-maximums, Table 1; Scherrer's method²⁰) indicates that the average crystallite size of air-prepared $\text{Co}^{\text{II}}\text{Co}^{\text{III}}\text{AlO}_4$ spinel matrix is about $5\text{--}8\text{ nm}$ [using (220) and (311) peaks of the spinel phase, respectively], noting that the nitrogen-prepared oxide sample is largely amorphous, although the same two peaks can still be recognized. Nanocarbons in the sulfate-functionalized carbon/metal-oxide nanocomposites can be observed with the HRTEM method after an acid separation. Some representative HRTEM images are shown in Figure 4. As can be seen, the carbon phase contains multiwalled CNPs with an average interwall distance (d_{002}) of $0.34\text{--}0.35\text{ nm}$; several to 40 graphene layers are observed in these CNPs. In general, they have short tube lengths of 20 to 100

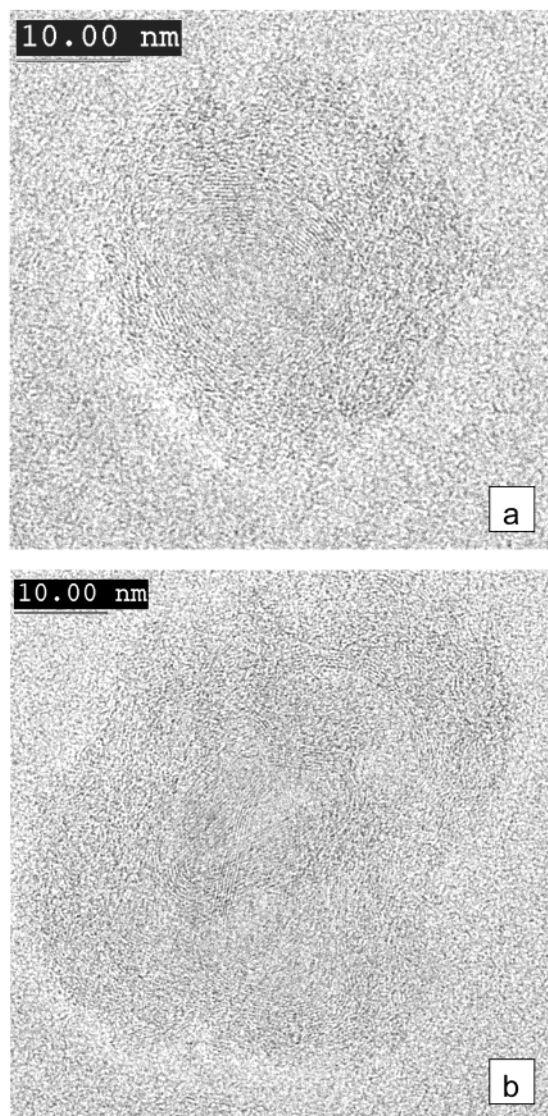


Figure 4. Representative HRTEM images of CNPs separated from nanocomposites (heated in nitrogen) via acid treatment: (a) a bucky onion and (b) an assembly of polyhedral CNTs.

nm with outer diameters in the range of 10 to 35 nm. Other morphologies of CNPs have also been observed, such as oval-shaped, polyhedral, and onion-like fullerenes that are commonly observed in vapor-phase growths.^{21,22} One important finding in this work is that the nanocarbons all have empty cavities (fullerene-type), which had not been reported in previous reports for the thermal degradation of MgAl-hydratalcites.³ The formation of these fullerene-based nanocarbons can be attributed to the confinement effect of the hydratalcite-like structure, which could be a crucial factor in the first step of the carbonation process. Furthermore, it should be mentioned that there have been many chemical techniques to open the fullerene-like caps of the CNPs.¹¹ If desired, the nano-cavity of CNPs can be further opened with a suitable oxidizing reagent.¹¹

As reported in Table 2, the chemical composition of the final nanocomposites depends strongly upon the processing method and intercalated anionic species. For example, the carbon content (and thus CNPs) is generally higher when

Table 2: Results of Elemental Analysis (in weight percentage) for the Nanocomposites Prepared at 400 °C for 2 h

| heating condition | C% | H% | N% | S% |
|----------------------|-------|-------|-------|--------|
| calcined in air | 8.003 | 1.418 | 0.680 | 11.355 |
| calcined in nitrogen | 8.934 | 0.934 | 0.363 | 10.754 |

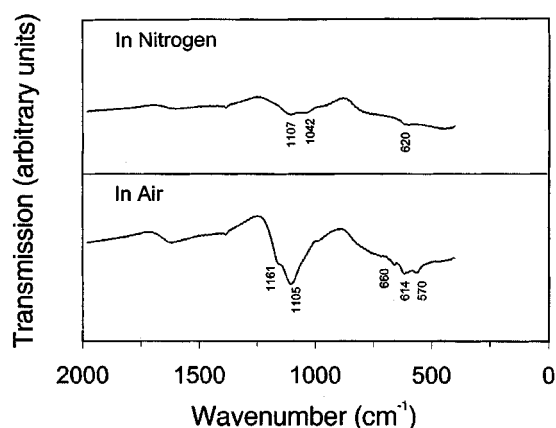


Figure 5. FTIR spectra for the sulfate-functionalized carbon/metal-oxide nanocomposites after heating the (poly)vinyl sulfonate–HTlc sample respectively in air and nitrogen at 400 °C for 2 h.

using the inert atmosphere. One important feature in this synthetic technique is that further chemical modification of composites can be achieved by introducing functional groups to the intercalated anions, such as the $[-SO_3^-]$ in the vinyl sulfonate anion for the present case. In catalytic applications, incorporation of SO_4^{2-} into metal oxide matrices (such as ZrO_2 and Al_2O_3) is often desired to generate greater acidity for the shape selective composites.^{9,10} With the intercalation of (poly)vinyl sulfonate anions, the sulfur content in the composites is still high even after heating at 400 °C. The FTIR study in Figure 5 further confirms the existence of sulfate ions SO_4^{2-} in these heated samples, where wavenumbers at 1161 and 1105 cm^{-1} are assigned to the splitting of ν_3 mode of SO_4^{2-} and 614 cm^{-1} to the ν_4 mode of the same anions,²³ while 660 and 570 cm^{-1} are attributed to M–O vibrational modes in spinels.^{15,16}

Surface analysis with XPS shows that in addition to the formation of $-C-O-$ (C 1s, BE = 286.3 eV) and $-COO-$ (C 1s, BE = 288.5 eV) species,^{24,25} both cobalt (two components of Co 2p_{3/2} at BE = 782.0 and 784.5 eV respectively) and sulfur (S 2p at BE = 169.3 eV) are found on the CNPs. Clearly, the external surfaces of CNPs in the latter case are also modified with SO_4^{2-} that are connected to the cations in cobalt sulfate (Co 2p_{3/2}, BE = 784.5 eV), noting that the $Co^{II}Co^{III}AlO_4$ spinel species is also found in the surface region (Co 2p_{3/2}, BE = 782.0 eV).^{17,24} It is believed that the presence of SO_4^{2-} and thus electrostatic attraction on the surface is the cause for the cobalt cation retention on the CNPs.

We have reported several unique features of this single-step synthesis of carbon/transition-metal-oxide nanocomposites. Nonetheless, the further work in design and control of the porous structure and chemical reactivity remains

challenging. For example, the selection of polymeric anions with desired functional groups may be crucial to form active catalysts to meet a specific chemical reaction. On the other hand, the type of polymeric anions may be another important synthetic factor controlling the final nanocarbon formation, together with the transition metal cations chosen in the brucite-like layers.

In summary, hydrotalcite-like compounds can be utilized as precursor materials for direct synthesis of hybrid nanocomposite materials. In particular, desired organic phases can be derived from the intercalated anionic species in the inter-layer space. Furthermore, functional groups can be introduced to nanocomposites by selecting functionalized anions such as $[-CH_2CHSO_3^-]_n^{n-}$ in the present study. Inorganic phases such as metal oxides, on the other hand, can be converted from the brucite-like layers after thermal decomposition. As a large variety of transition metals possess divalent state, chemical composition of the brucite-like layers and thus the decomposed oxides can be designed with great flexibility.

Acknowledgment. The authors gratefully acknowledge research funding (RP3999902/A and A/C50384) co-supported by the Ministry of Education and the National Science and Technology Board of Singapore.

References

- (1) Cavani, F.; Trifiro, F.; Vaccari, A. *Catal. Today* **1991**, *11*, 173.
- (2) (a) Reiche, W. T. *Solid State Ionics* **1986**, *22*, 133. (b) Rives, V.; Ulibarri, M. A. *Coord. Chem. Rev.* **1999**, *181*, 61.
- (3) (a) Oya, A.; Mita, H.; Otani, S. *Appl. Clay Sci.* **1990**, *5*, 13 and references therein. (b) Hibino, T.; Kosuge, K.; Tsunashima, A. *Clay Clay Mineral.* **1996**, *44*, 151.

- (4) Faure, C.; Borthomieu, Y.; Delmas, C.; Fonsassier, M. *J. Power Sources* **1991**, *36*, 113.
- (5) Armor, J. N.; Braymer, T. A.; Farris, T. S.; Li, Y.; Petrocelli, F. P.; Weist, E. L.; Kannan, S.; Swamy, C. S. *Appl. Catal. B* **1996**, *7*, 397.
- (6) Hermosin, M. C.; Pavlovic, J.; Ulibarri, M. A.; Cornejo, J. *Water Res.* **1996**, *30*, 171.
- (7) Chisem I. C.; Jones, W. J. *Mater. Chem.* **1994**, *4*, 1737.
- (8) Xu, Z. P.; Zeng, H. C. *J. Phys. Chem. B* **2000**, *104*, 10206.
- (9) Coq, B.; Planeix, J. M.; Brotons, V. *Appl. Catal. A* **1998**, *173*, 175.
- (10) Yadav, G. D.; Nair, J. J. *Chem. Commun.* **1998**, 2369.
- (11) Ajayan P. M.; Ebbesen, T. W. *Rep. Prog. Phys.* **1997**, *60*, 1025 and references therein.
- (12) Subramoney, S. *Adv. Mater.* **1998**, *10*, 1157 and references therein.
- (13) Drezdson, M. A. *Inorg. Chem.* **1988**, *27*, 4628.
- (14) Oriakhi, C. O.; Farr, I. V.; Lerner, M. M. *J. Mater. Chem.* **1996**, *6*, 103.
- (15) Xu, Z. P.; Zeng, H. C. *J. Mater. Chem.* **1998**, *8*, 2499.
- (16) Chellam, U.; Xu, Z. P.; Zeng, H. C. *Chem. Mater.* **2000**, *12*, 650.
- (17) Ji, L.; Lin, J.; Zeng, H. C. *J. Phys. Chem. B* **2000**, *104*, 1783.
- (18) *Carbon Nanotubes*; Endo, M., Iijima, S., Dresselhaus, M. S., Eds.; Pergamon: Oxford, 1996.
- (19) Saito, R.; Dresselhaus, G.; Dresselhaus, M. S. *Physical Properties of Carbon Nanotubes*; Imperial College Press: London, 1998.
- (20) Cheetham, A. K.; Day, P. *Solid-State Chemistry: Techniques*; Clarendon Press: Oxford, 1987; p 79.
- (21) (a) Saito, Y. In *Carbon Nanotubes*; Endo, M., Iijima, S., Dresselhaus, M. S.; Eds.; Pergamon: Oxford, 1996; p 153. (b) Ugarte, D. In *Carbon Nanotubes*; Endo, M., Iijima, S., Dresselhaus, M. S., Eds.; Pergamon: Oxford, 1996; p 163.
- (22) Ji, L.; Lin, J.; Zeng, H. C. *Chem. Mater.* **2000**, *12*, 3466.
- (23) Nakamoto, K. *Infrared and Raman Spectra of Inorganic and Coordination Compounds*, Part A., 5th ed.; John Wiley & Sons: New York, 1997; p 199.
- (24) Moulder, J. F.; Stickle, W. F.; Sobol, P. E.; Bomben, K. D. In *Handbook of X-ray Photoelectron Spectroscopy*; Chastain, J., Ed.; Perkin-Elmer Corporation: MN, 1992.
- (25) Barr, T. L.; Seal, S. *J. Vac. Sci. Technol. A* **1995**, *13*, 1239.

NL010045D